

We are IntechOpen, the world's leading publisher of Open Access books Built by scientists, for scientists

6,900

Open access books available

186,000

International authors and editors

200M

Downloads

Our authors are among the

154

Countries delivered to

TOP 1%

most cited scientists

12.2%

Contributors from top 500 universities



WEB OF SCIENCE™

Selection of our books indexed in the Book Citation Index
in Web of Science™ Core Collection (BKCI)

Interested in publishing with us?
Contact book.department@intechopen.com

Numbers displayed above are based on latest data collected.
For more information visit www.intechopen.com



Environmental Gamma-Ray Observation in Deep Sea

Hidenori Kumagai, Ryoichi Iwase, Masataka Kinoshita,
Hideaki Machiyama, Mutsuo Hattori and Masaharu Okano
JAMSTEC (Japan Marine Science and Technology Center,
Japan Agency for Marine-Earth Science and Technology)
Japan

1. Introduction

Deep-Sea *in-situ* radioactivity measurements were initiated in 1964 for investigation of sunken USN atomic power submarine Thresher by using Geiger counters (Wakelin, 1964). Since then, *in-situ* radioactivity monitoring utilizing a towed-fish and/or remote sea bottom stations has been carried out in various countries. But they are mainly used for surveys of artificial radio activities to evaluate potential risks around atomic power plants, radioactive waste disposal sites and sunken nuclear objects etc. (Jones et al., 1988). Thus, underwater gamma ray measurement has been rather limitedly performed compared to the sub aerial ones, which has been widely utilized for explorations of uranium or other valuable minerals for mining or much wider environmental analysis (Bristow, 1983), due to very effective shielding by seawater. In underwater environment, Yoshida and Tsukahara (1987) reported environmental gamma ray characteristics around an active cold seepage associating with an active fault in Sagami Bay, southern coast of mainland Japan. Besides that, deep-sea gamma ray surveys for scientific use are intensively carried out by ODP-IODP logging for determination of rock types.

This chapter intends to demonstrate some usage of environmental gamma-ray measurement, through the studies in the deep sea environment, e.g. deep sea hydrothermal vent, cold seeps, active faults. Further, this chapter also tries to document relationship with tectonic settings and geological events. For this purpose, the specification and assemblage of the gamma ray sensor systems of JAMSTEC are introduced firstly. Next, an examples of the field measurement will be shown as a temporal variation that reflecting the uniqueness of deep sea. Although the sensitivities of the current model of sensor are significantly reduced by the thick Al or Ti pressure hull to endure high pressure in deep sea, the collected gamma ray spectra and distributions of intensities indicated some linkages with tectonic settings to date.

2. Instrumental

The apparatus collected to the world-wide gamma ray spectra in the deep sea environment, through hundreds dives of manned submersibles Shinkai6500/2000 and Remotely Operated

Vehicles (ROVs). In addition, an on-line real-time environmental gamma ray observatory has operated at deep seafloor of 1174m water depth for more than ten-years at Hatsushima Observatory, Sagami-Bay, southern coast of mainland Japan.

All the deep-sea systems developed are based on an on-land system originally developed at RIKEN (the Institute of Physical and Chemical Research; Okano et al., 1980; Kumagai and Okano, 1982). Since 1984, Deep-Sea Research department of JAMSTEC had developed deep-sea gamma ray sensor available down to 6500m of water depth (Hattori et al., 1997; 2000; 2002). To achieve required sensitivity for the system, NaI(Tl) scintillation counter has applied to the measurement that stored into Al-pressure vessel (Plate 1). Figure 1 is a schematic block diagram of the system. During the development, various assemblages of high voltage supply, data transfer, and sizes or shapes of scintillator were tried; three or two inches spherical, or three inches cylindrical scintillators. As the current model, three inches



Plate 1. Deep sea gamma-ray sensor for a manned submersible *Shinkai6500*. NaI(Tl) scintillator are in the Al-pressure container (dark green colour, wrapped by black plastic tape, left). Under an operation, the sensor unit is connected through an underwater connector on the pressure container (silver coloured cover) to a feed-through on the pressure hull of submersible by underwater cable. The data signals are transferred to PC via power supply box (silver coloured) where +12V DC power is converted from AC power supplied from submersible to feed to the sensor unit.

spherical NaI(Tl) scintillator has been adopted and stored into Al-pressure container with high voltage supply and with multi-channel pulse height analyzer (PHA). The power supply for the underwater part is +12 V or +24 V according to the specifications of platforms (submersibles, towed-fish, etc.). When the γ -ray was detected by the system, its energy level was determined by PHA and transferred via serial communication of 9600 baud of RS-232C. Under this constraint, the channels of PHA are limited to 256. Firstly, the system was equipped on a towed-fish (Deep-tow system) and then applied on submersibles and other platforms, including a real time observatory (Hattori et al., 2000; Iwase et al., 2001). The approximate sensitivity of the apparatus is 0.25 nGy/h/cps, which is significantly reduced by the shielding by their pressure vessels.

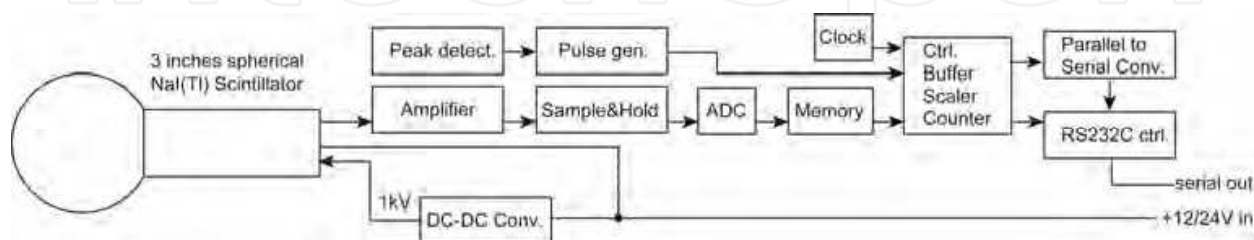


Fig. 1. Schematic block diagram of the Deep-sea gamma-ray sensor.

Once NaI(Tl) scintillation system rolled out, Ge-semiconductor detector had also tried to use. Instead of its high resolution to resolve the energy distribution of γ -ray radiations in environment, the sensitivity of Ge-semiconductor system is one-third or one order lower than that of NaI(Tl) scintillation system. Thus, the Ge-semiconductor system has limited to a trial production in JAMSTEC although another institutions, e.g. Japan Atomic Energy Research Institute (JAERI), tried further development for environmental monitoring (Ito et al., 2005).

2.1 Protocols of analysis

In analysis, the peel-off (stripping) method is applied to resolve the contributions from different nuclides to the total gamma-ray intensity. The method identifies the total energy peaks from approx. 3MeV to lower. In this energy region, the scintillation spectra are composed of photopeaks and their Compton continuums. Here, each of Compton continuums is assumed to have flat distribution. Thus, to resolve the photon energy distribution, the Compton continuums were sequentially peeled off from higher energy level to lower (Okano et al., 1982). These protocols are partly available on commercial applications, e.g. Seiko EG&G Co. Energy calibrations are performed for all time-series data typically for individual dives by using frequently identified three photopeaks: 609 keV of ^{214}Bi , 1460 keV of ^{40}K and 2614 keV of ^{208}Tl .

3. Intensities of gamma-radiation in seawater and on seafloor

Due to the effective shield by seawater, total count rate in water is rather lower than that of sub aerial measurement (Yoshida and Tsukaraha, 1987). According to the geological environment, total count rate of sub aerial environment is 20-100 nGy/h in Japan, which is equivalent to approx. 80-400 counts per second (cps) in our system: 1 nGy/h is equivalent to 4cps. Figure 2 is an example of the time-series record of total count rate in submersible dive:

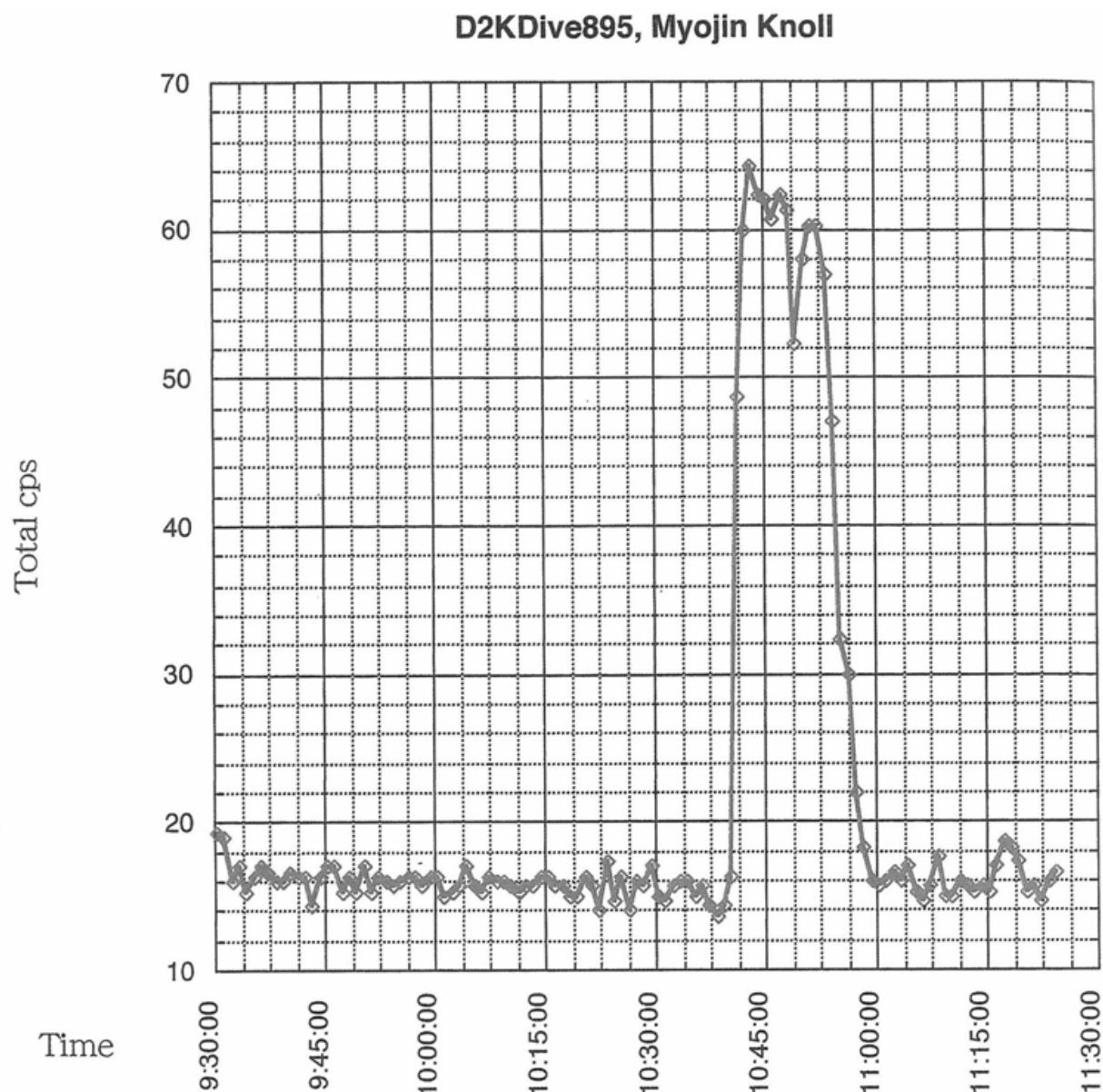


Fig. 2. A typical time sequential record obtained by submersible dives; 895th dive of *Shinkai2000* at Myojin Knoll, Izu-Bonin Arc. Original Fig. was in Hattori & Okano (1999).

collected at the 895th dive of *Shinkai2000*. The cosmic-ray induced high energy gamma ray, $> 3\text{MeV}$ as its energy level, still penetrate into shallow water, which raises total count rate approx. 20 cps. Descending to deeper, the total count rate decreases down to 10 cps or lower in typical; in this example, the minimum count rate is approx. 14 cps. In the area with little suspended material in water column, such a minimum decreases down to 5 cps, e.g. in the vicinity of Mid Atlantic Ridges (Hattori et al., 2001). Approaching to the seafloor, total count rate raises up again to a few tens cps in most cases, which indicate significant contribution from seabed. Figure 3 shows the distributions of the maximum total count rates recorded when submersibles or ROVs were on bottom, touching on the seabed. The mode of the recorded value is in the class of 10-20 cps in linear scale with 10 cps in intervals, however, the frequency of the count rate gradually decreases to much higher count rate; there is no significant gap in the distribution. Even in this context, the area around the hydrothermal

vents or cold seeps associated with active fault showed significantly anomalous count-rate, up to 10^4 cps; the highest total count rate was recorded at Izena Hole caldron, >8900 cps. Other hydrothermally active areas also showed rather high count-rates, e.g. Iheya ridges, Hatoma-knoll, Ishigaki-knolls of Nansei-shoto and Kagoshima-bay (Southwest Japan), Myojin-knoll of Shichito-Iwojima Ridge. To judge the apparent anomaly from the above described general distribution, here after 100 cps is adopted as a tentative threshold to identify geological activities. Here also pseudo-logarithmic scales were applied in Figure 3b to show the entire variation of total count-rate. In this figure, distribution peak of the γ -ray intensity is on the class 50-100 cps, which also support this tentative threshold.

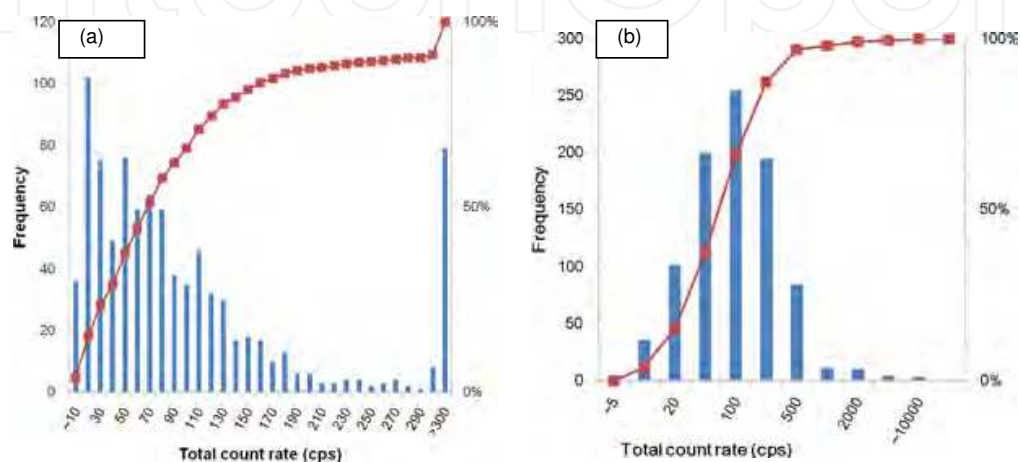


Fig. 3. Maximum total count rate distribution recorded at individual dives of submersibles: (a) Linear scale classification of every 10 cps in intervals, (b) Data classification under logarithmic-like scale. Blue bars: frequency in the class; Red sequential line: cumulative relative frequencies from lower count rates.

3.1 Relationships between tectonic settings and gamma-ray signature

Hereafter, some examples of the intensities of environmental γ -ray obtained in various geological settings are discussed. Figure 4 summarizes the measured distributions of total count rate maxima of γ -radiation around Japan. It is clear that the anomalous values were recorded all the area around Japan even in the area rather old geologic edifices; e.g. Komahashi-daini Knoll of Kyushu-Palau Ridge, or Annei Smt. of Nishi-Shichito Ridge.

The localities where very high count-rates were observed, > 1000 cps, were limited to the active hydrothermal sites developing on the arc-backarc volcanoes: volcanism developing above trench-arc system relating to seafloor subduction. In contrast to the hydrothermal sites, fore-arc cold seepages showed moderately high count-rates, up to 500 cps; mostly not exceeding to 200 cps. It is notable that four of five localities where the very high count-rate recorded (>1000 cps) were in Okinawa Trough. It is a back arc basin developing between Nansei-Shoto and Asian continent in East China Sea, where thick terrigenous sediments have been accumulated. Generally, major radioactive elements, K, Th and U^1 , are rich in

¹ All these elements are geochemically classified to incompatible elements that concentrated into continental crust due to their incompatibility to the rock forming minerals. Thus, oceanic crust or magmas in ocean are relatively poor in such elements.

such terrigenous sediments, which potentially cause the high count-rate of γ -radiation. The hydrothermal circulation within the sedimentary layer enhanced by the magmatic heat sources may scavenge and concentrate such radioactive species from thick sediments in those areas. Therefore, it is natural that the hydrothermal activities in oceanic environment far from continents or large land masses, e.g. at Mid-Ocean Ridges, did not show any very high count-rates. The vicinity of Hawaiian Island is also the area of low γ -ray intensities. In those areas, maximum count rates did not exceed 200 cps.

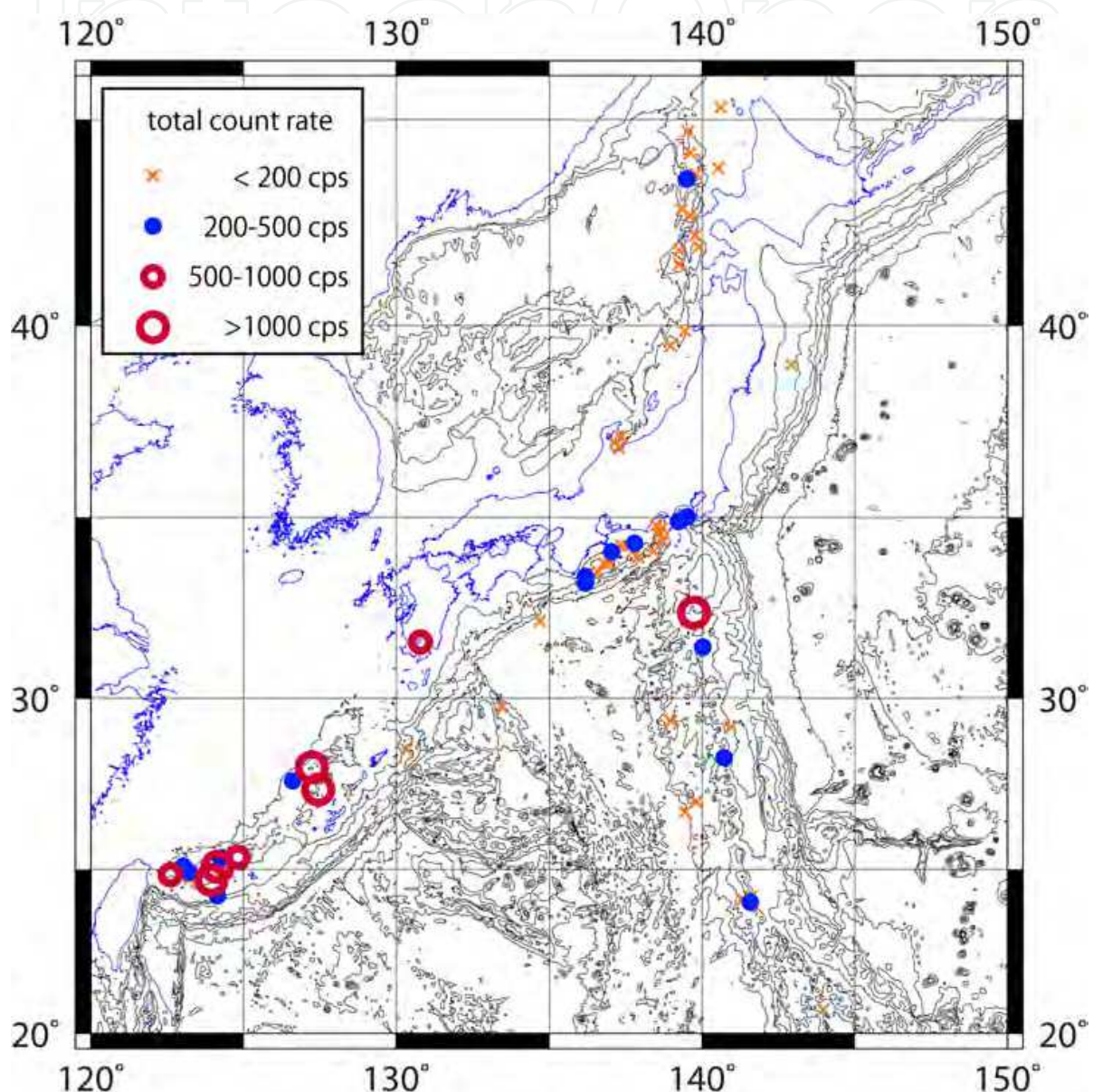


Fig. 4. The regional distribution of anomalous total count rate maxima, 100 cps, in the vicinity of Japan. Bathymetric contours are drawn as 1000 m in intervals. Original figure was taken from Hattori & Okano (2002) and redrawn.

Even by using NaI(Tl) scintillator with 7% resolution, the sources of γ -ray could be resolved by its energies. In this purpose, three characteristic γ -ray of 609 keV of ^{214}Bi , 1460 keV of ^{40}K and 2614 keV of ^{208}Tl were used in this study. Under some reasonable assumptions, either

radiation dose rate or concentrations of γ -ray source nuclei in the environment could be calculated. Hereafter the radiation dose rates are applied because it is not obvious the spatial distribution of the source nuclei at the various locations; geometric complexities of the seafloor having tall hydrothermal chimneys abruptly standing up > 10m in some cases and contribution from vigorous flow out from hydrothermal chimneys or seepages may cause unexpected increase of gamma radiation.

Figure 5 shows the statistics of γ -ray dose rate from three possible sources, K, U-series and Th-series, respectively. K is major element in seafloor sediment; the recorded maximum of dose rate was 7.0 $\mu\text{R}/\text{h}$ regardless of its mode at 0.28 $\mu\text{R}/\text{h}$. Entire variation was within three orders of magnitude, which was narrower than those of U- and Th-series radiations (Figure 5(a)).

Contrary to K, dose-rate of U-series varies more than five orders of magnitude caused by its maximum of ~ 200 $\mu\text{R}/\text{h}$ regardless of its relatively low mode (0.54 $\mu\text{R}/\text{h}$; Figure 5(b)). Dose rate distribution of Th-series shows the intermediate nature between K and U-series, ranging within four orders of magnitude (Figure 5(c)). It is notable that its mode of distribution is 1.38 $\mu\text{R}/\text{h}$, which is much higher than that of U-series. It may relate to the rather broad distribution tailing to the higher side of dose rate. This nature will be discussed later.

Under comparison with the recorded enormous total count-rate and the large variation of U-series dose rate, high concentration of U-series in environment should cause very high intensities of γ -ray, > 1000 cps, equivalent to >250 nGy/h. To confirm this view, the relationship of total count rates with U-series dose rate is plotted in Figure 6. It is clear that the observed high count rates were tightly associated with the high dose rate of U-series, > 100 cps as total count rate. Considering the progeny radio-nuclei of U-series and their half lives, Ra fed from hydrothermal vent fluids causes such radio activities². Even in the lower count-rate environment, rough relationship between total count rate and U-series dose rate still found, which suggests a ubiquity of U-series controlled γ -radiation environment; that is represented by the areas of hydrothermal activities in the higher dose rate end of correlation line. In addition, the trends was slightly above from the extrapolation defined in >100cps of total count rate. It is suggested significant contributions caused from Th-series nuclei, which built up the total count-rate.

To investigate such Th-series contribution, measured dose rates of U-series and Th-series were plotted (Figure 7). As predicted the above described relationship between total count rate and U-series dose rate, the data were dominantly plotted around the correlation line of slope 1. This also supports the view of a ubiquity of U-series controlled γ -radiation environment. Above the trend, a few tens of data obtained from the fore-arc seepage areas were plotted; e.g. in Suruga Bay or in Sagami Bay (both are in southern coast of mainland Japan), or off Kamaishi-city near the Japan Trench. In such areas, the U-series dose rate is not so high regardless of the moderately high total count rate, up to 300 cps. Instead, dose rate of Th-series reaches approx. 5 $\mu\text{R}/\text{h}$ regardless of the dose rate of U-series of <1 $\mu\text{R}/\text{h}$. As these areas are in the vicinities of active faults, thus, the contribution from Th-series nuclei is significant in the tectonics controlled environment. The data points from other tectonic active area either on southern coast of mainland Japan (e.g. Zenisu-ridge) or in

² Ra is in the group of an alkaline earth elements, which shows high solubility to water. Ra also frequently replaces Ba in minerals as the same group element.

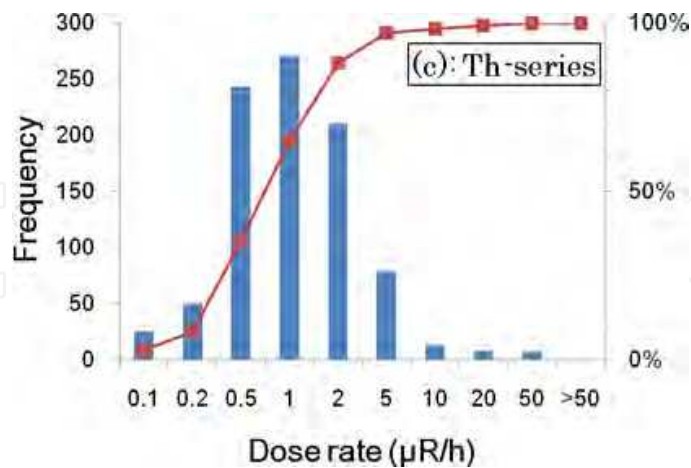
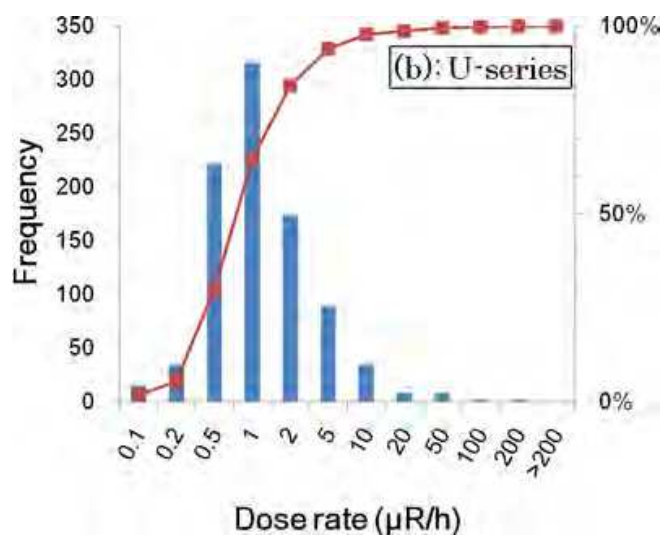
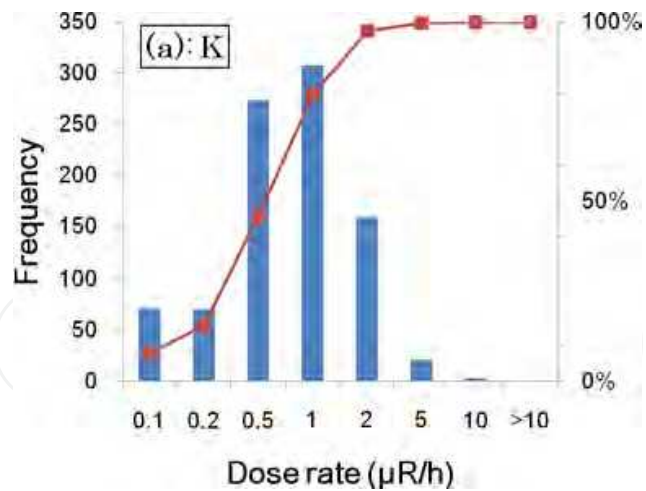


Fig. 5. The maximum dose rate distribution of individual sources; (a): K, (b): U-series, and (c): Th-series.

Japan sea-side (e.g. off Rebun Isl.) are also plotted above the line regardless of rather lower total count rates. These signatures may relate to squeezing of pore fluids by the compaction of sediments, which supplies Ra or other soluble species in seafloor environment.

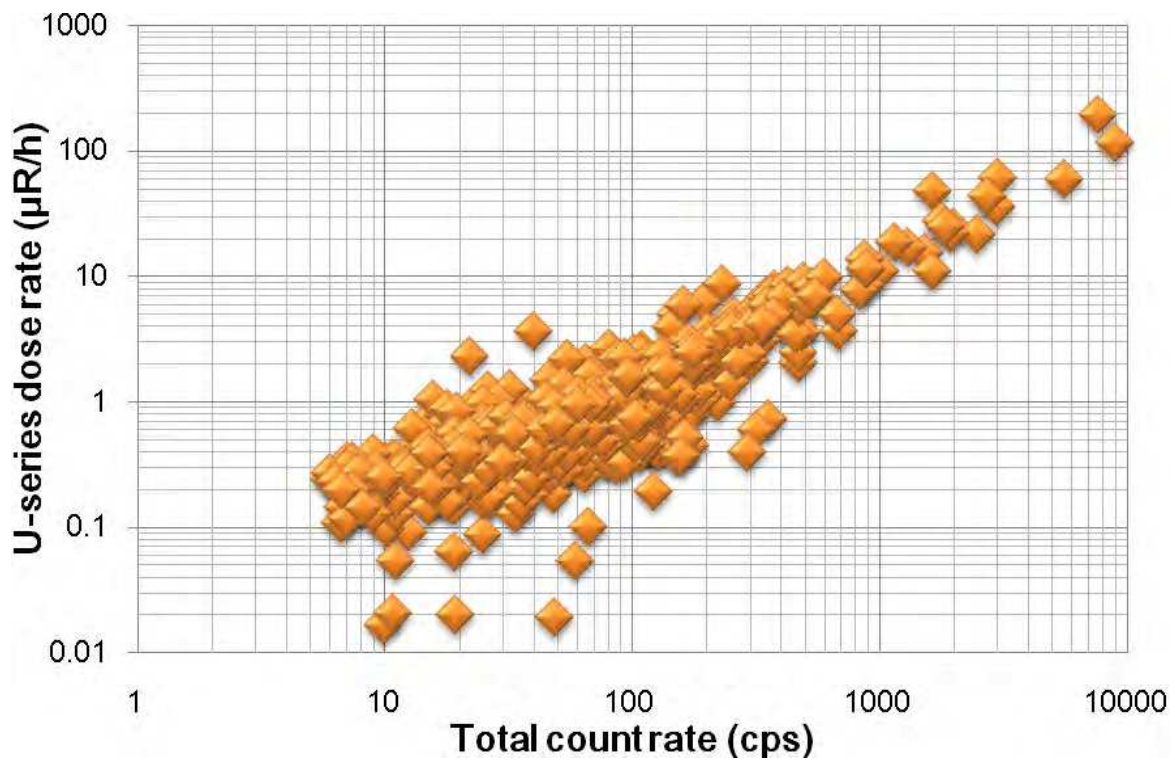


Fig. 6. The relationship between maximum total count rate and maximum dose rate from U-series nuclei. Most of data were tightly scattered around slope-1 correlation line.

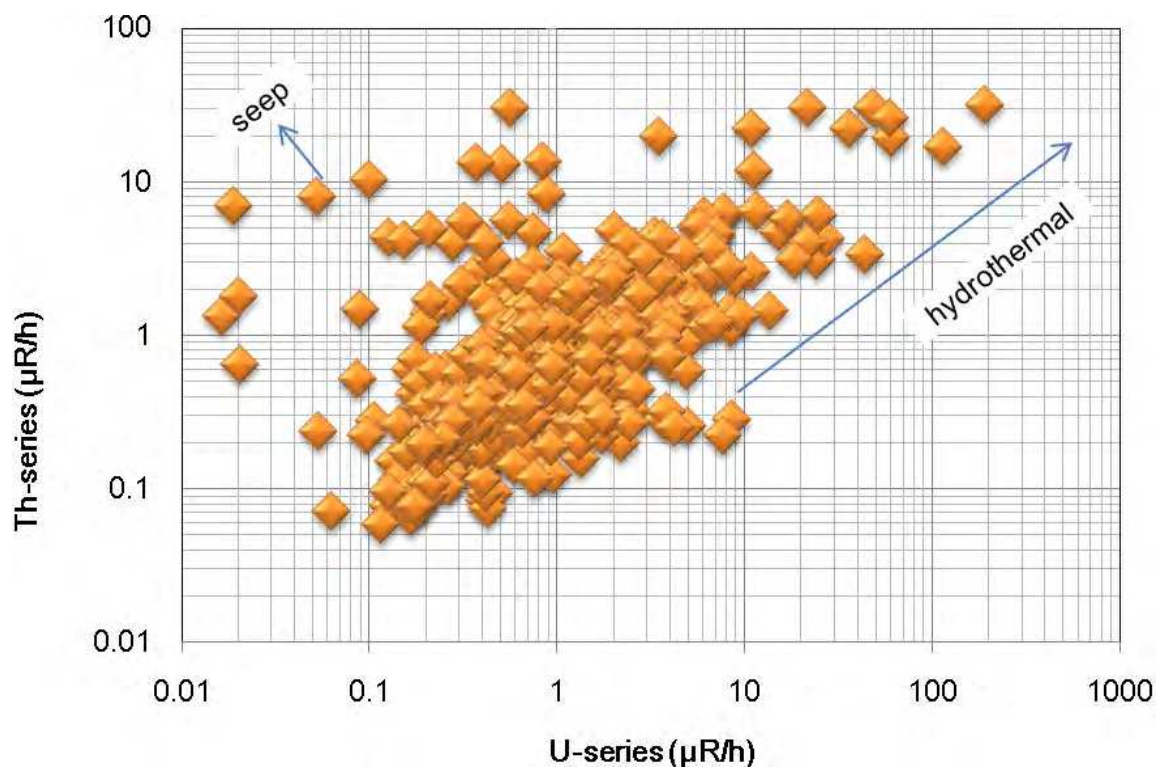


Fig. 7. The relationship of maximum dose rate from U-series and Th-series nuclei. Above the dense data distribution well correlate with U-series increase, a few tens of relatively high Th-series dose rate data were found.

3.1.1 Environmental gamma radiation in Mid-Ocean Ridges

In Figure 7, several points of moderately high Th-series contribution but very little U-series contributions are found: $>1 \mu\text{R/h}$ and $< 0.1 \mu\text{R/h}$ of respective Th-series and U-series dose rate. These data came from Indian Ocean either at the Rodriguez Triple Junction (RTJ) or at Atlantis Bank (AB). Those areas are well away from any continents or large land masses but very tectonic active area, thus very little terrigenous sediments accumulated. RTJ is a Ridge-Ridge-Ridge type triple junction where very slow spreading Southwest Indian Ridge (SWIR) is propagating toward the junction of Central Indian Ridge and Southeast Indian Ridge. The magmatic activity of SWIR is very low due to its very slow spreading, thus numbers of active faults developed in the area. AB is one of the Oceanic Core Complex³ that tectonically exposed and consisted of gabbros and peridotites. It locates $\sim 100\text{km}$ away from present-days ridge axis, but, it is regarded to be exposed tectonically near the ridge axis approx. 12 Ma. The gabbros are in the category of mafic plutonic rocks that usually contains very little radioactive nuclei. These relatively old age and the composition of seabed caused such low gamma radiations in the areas. These tendencies are in the context of the Th-series enrichment in tectonic active area.

4. Long term monitoring at Hatsushima station, Sagami-bay

JAMSTEC has been carrying out multi-disciplinary real time long term observation on deep seafloor at a depth of 1175 m off Hatsushima Island in Sagami Bay. There, a cabled observatory was deployed with several kinds of sensors e.g. video cameras, a CTD sensor that measures conductivity of seawater, ambient temperature and depth of water, a seismometer, since 1993 (Momma et al., 1998). The main target of the observatory is to investigate the environmental and biological phenomena of the cold seepages around the observatory that feed a large number of chemo-synthetic biological communities which are mainly consisted of Vesicomysid clam.

In March 2000, the original observatory, which had been deployed in September 1993, was retrieved and fully renewed. The renewed observatory and the submarine cable connected were deployed at the position of approximately 40 m northward from the original one (Iwase, 2004). At the renewal, a gamma-ray sensor with NaI(Tl) scintillator was attached to the observatory. Since then, a long term environmental gamma-ray monitoring was started. The renewed observatory was retrieved again in March 2002 to repair, and re-deployed in November 2002 approximately 40 m southward from the previous position had deployed; i.e. the observatory relocated into almost the same position where the original observatory had located. Then, gamma-ray observation has resumed and continued at the same position for almost 9 years to date.

The specification of the gamma-ray sensor equipped to the station is almost the same as those for submersibles or a ROVs of JAMSTEC: three inch spherical NaI(Tl) scintillation counter and 256-channel PHA. It is stored in a titanium container (Plate 2). The output signal with a 9600 baud RS232C interface is transmitted to the shore station in Hatsushima

³ Oceanic Core Complex (OCC) is a domy exposure of lower lithological units of oceanic plates. It is frequently observed along Mid-Ocean Ridges with slow spreading rate, e.g. Mid Atlantic Ridge or Southwest Indian Ridge.

Island through the electro-optical submarine cable. The energy spectra can be obtained by automated calculation every ten minutes at the shore station, i.e. each dataset of energy spectrum is the summation of ten minute measurement. The gamma-ray sensor unit is installed to touch its scintillator side on seabed in which scintillator is attached downward to maximize its sensitivity (Plate 3).

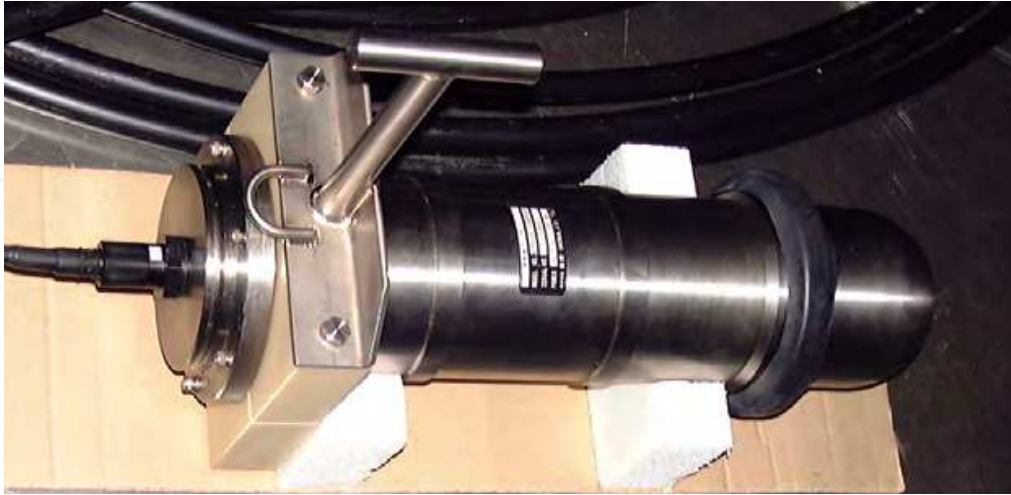


Plate 2. Gamma ray sensor of cabled observatory off Hatsushima Island.

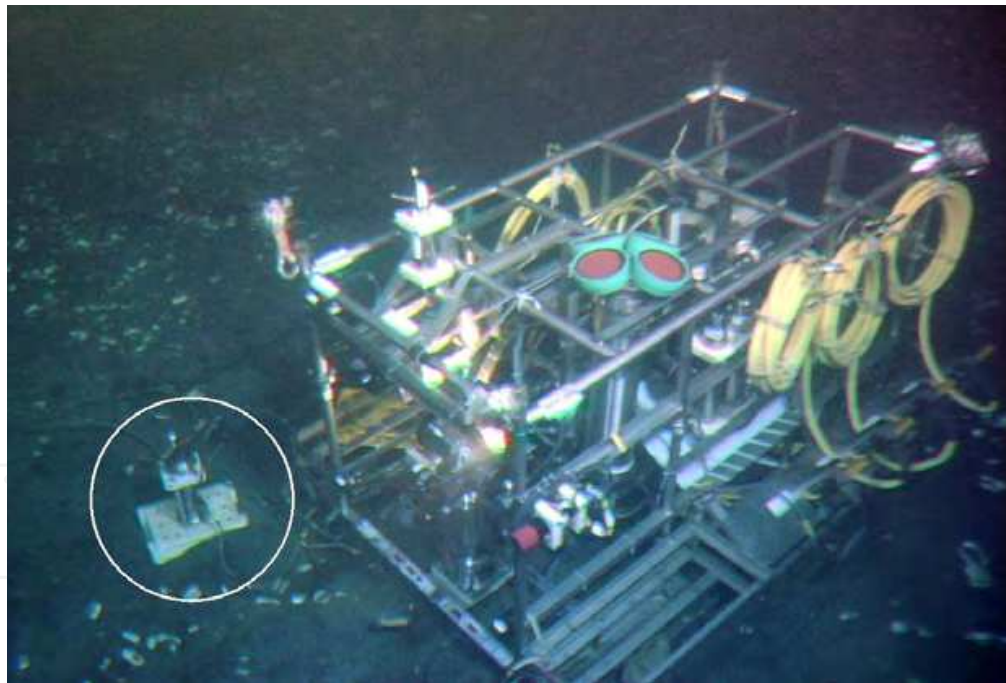


Plate 3. Cabled observatory off Hatsushima Island and gamma ray sensor (denoted by circle) deployed on seafloor.

It is known that output signal of NaI(Tl) scintillator is affected by temperature variation. However, since the water temperature at the observation site on deep seafloor is approx. 3 °C and shows very small perturbation, the influence with temperature is negligible. On the other hand, some kind of signal drift associated with aging could occur. Fig. 8 shows the spectra obtained on January 1st in 2003, 2005, 2007, 2009 and 2011. Each spectrum is

accumulated for one day. Prominent peaks of natural radiation ^{214}Bi , ^{40}K and ^{208}Tl are remarked. It is obvious that each peak linearly shifts to lower channel as time passes.

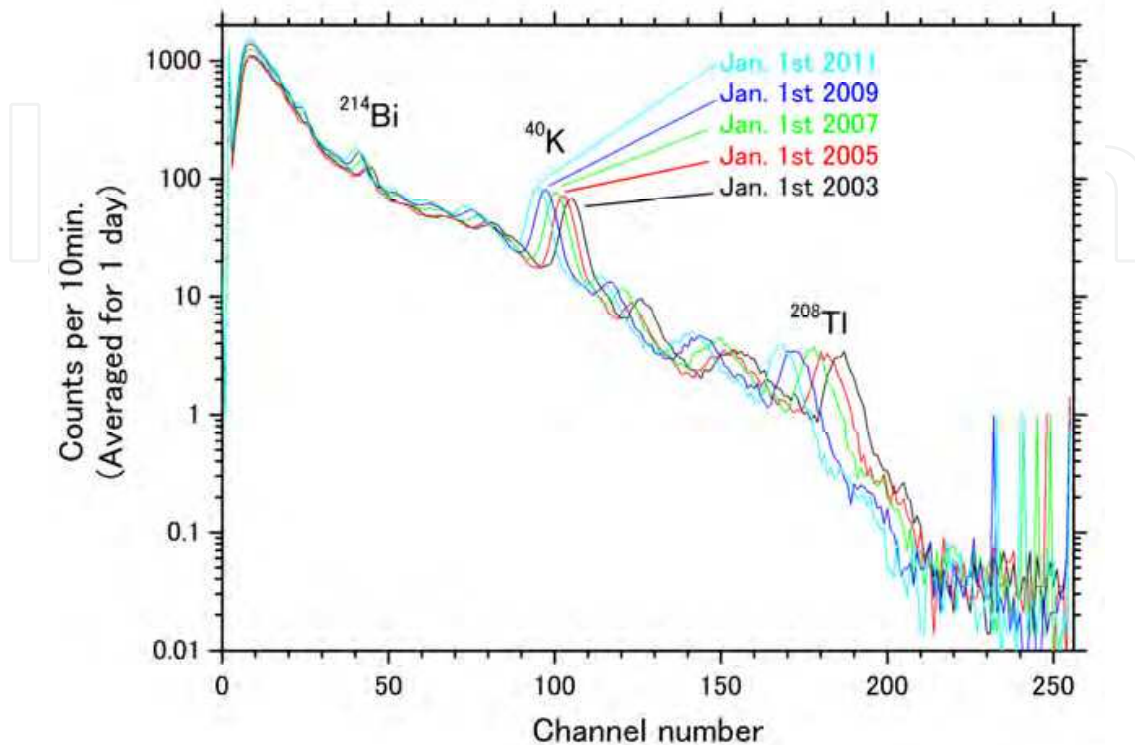


Fig. 8. Gamma ray energy spectra observed with the observatory.

The correspondence between channel number and energy was calibrated by using those three peaks (^{214}Bi of U-series, ^{40}K and ^{208}Tl of Th-series) in the one day averaged spectrum. The centre position of each peak was calculated by curve fitting. Fitting function is the combination of Gaussian and linear function as follows,

$$y = A \exp\left\{-4 \ln 2 \left[\frac{(x-p)}{\text{FWHM}}\right]^2\right\} + ax + b, \quad (1)$$

where x is channel number, y is the number of counts, A is the peak height, p is the centre position of the peak in units of fractional channel number, FWHM is the full width at half maximum of the peak in units of fractional channel number, a and b are the constant parameters.

As the result, the centre position of each energy peak decreased at roughly constant rate. In case of ^{40}K (1461 keV), the centre position of the peak decreased as large as 10 channels for the period of 8 years (Fig. 9), while the relation between the channel number and energy stayed linear (Fig. 10).

On the other hand, the full width at half maximum (FWHM) of each peak, which was calculated at the same time by the curve fitting, stayed almost constant as are shown in Fig. 11 (a)-(c) for ^{214}Bi , ^{40}K and ^{208}Tl , respectively.

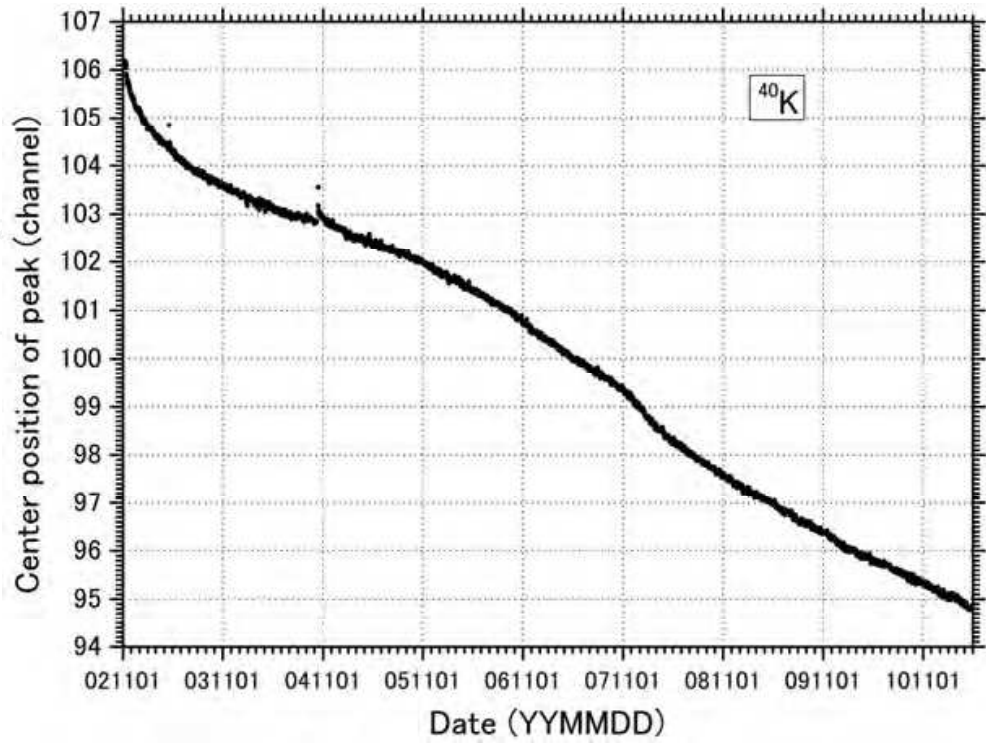


Fig. 9. Temporal change of the center position of ^{40}K peak.

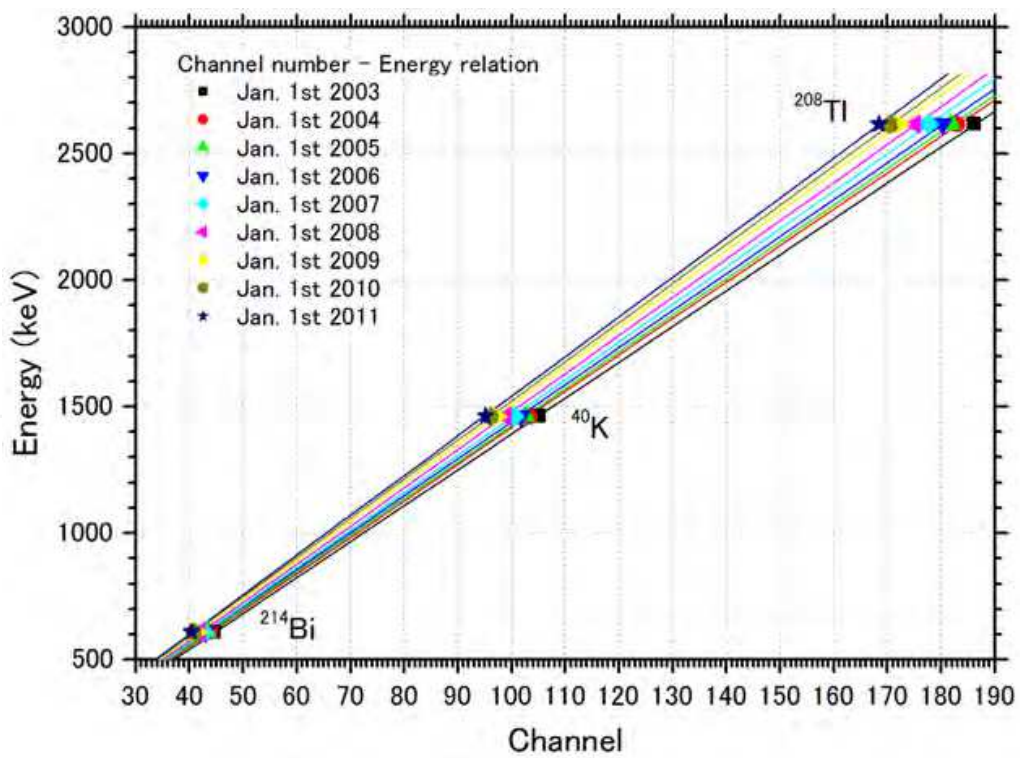
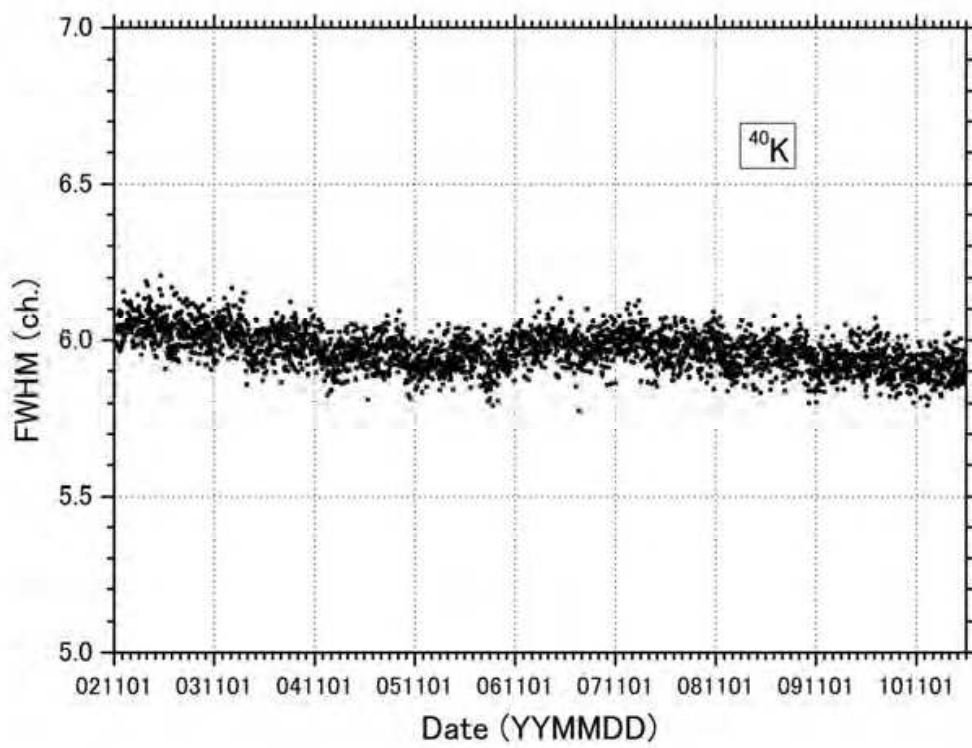
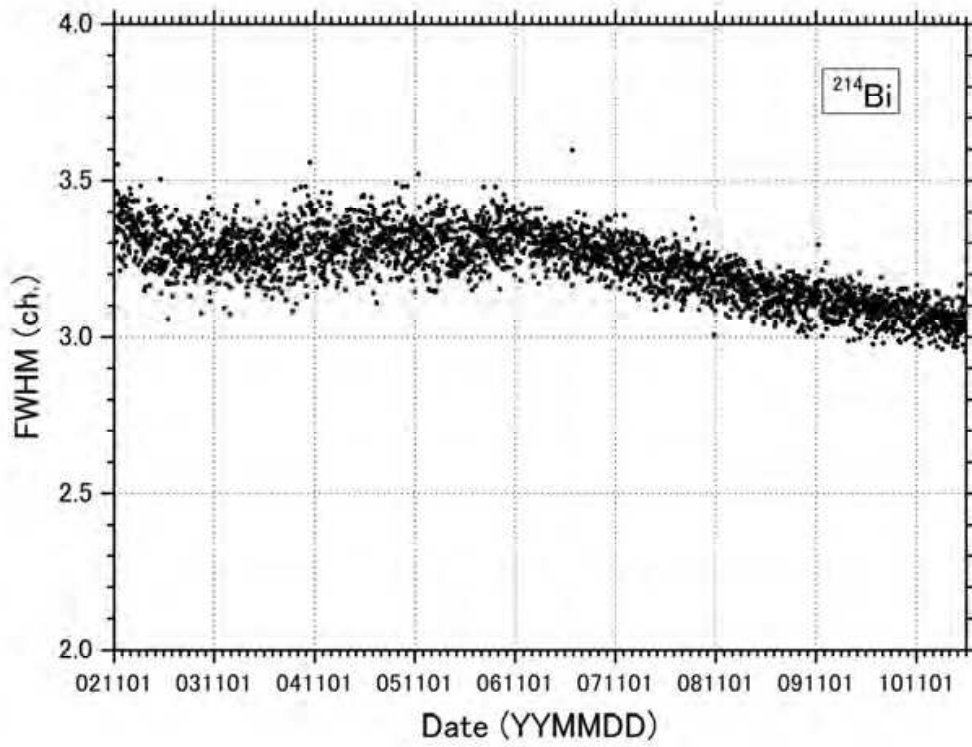


Fig. 10. Temporal change of relation between channel number and energy.



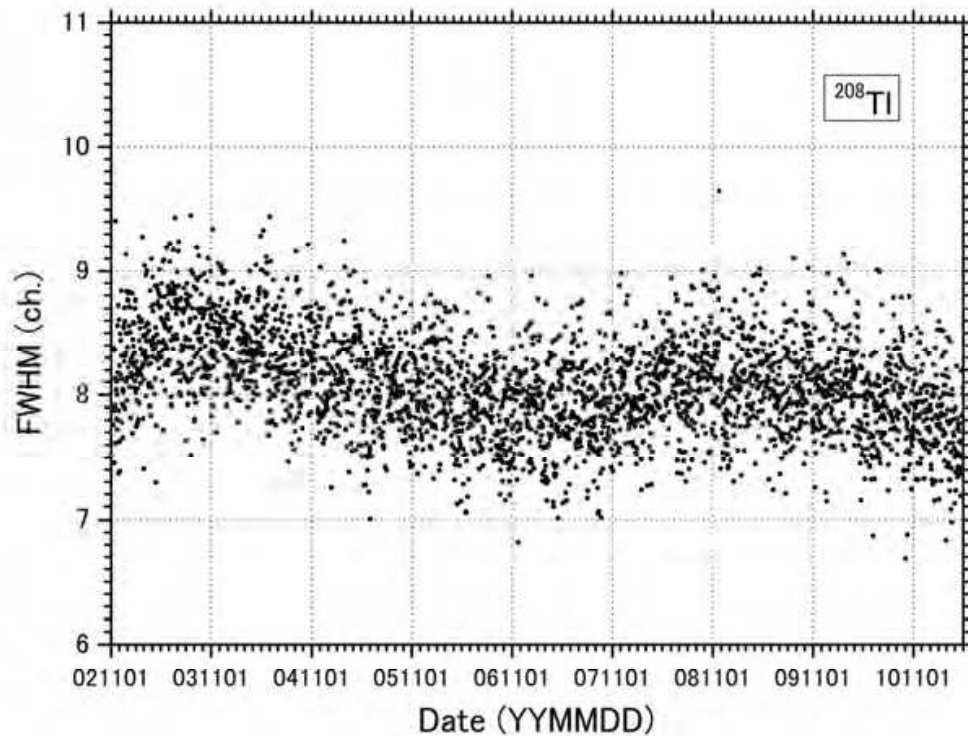
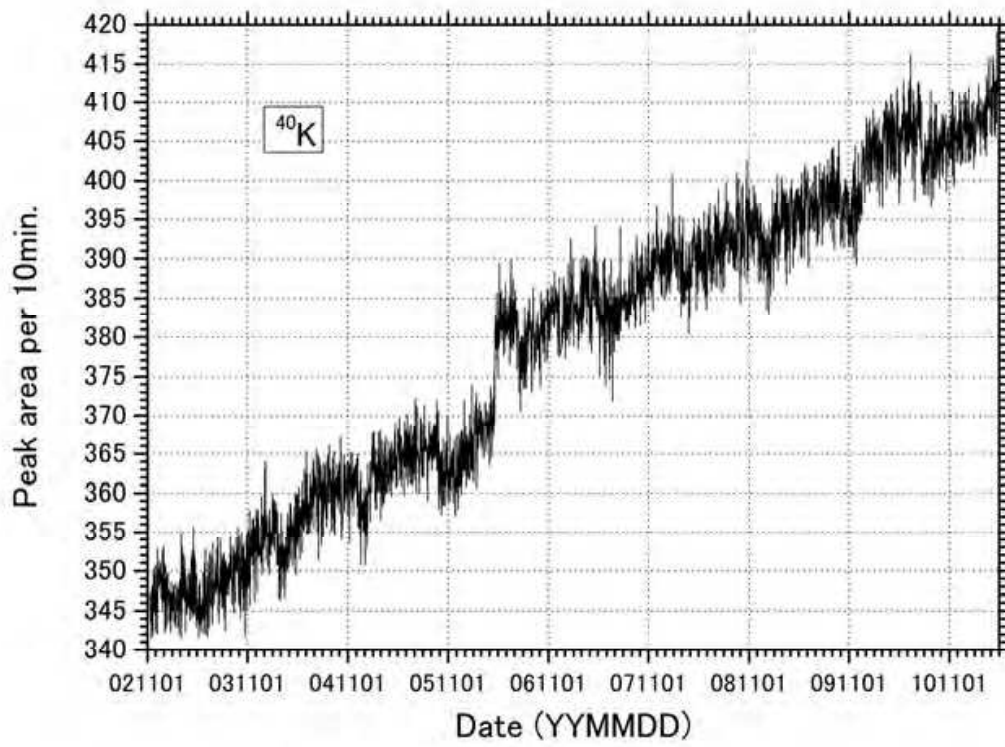
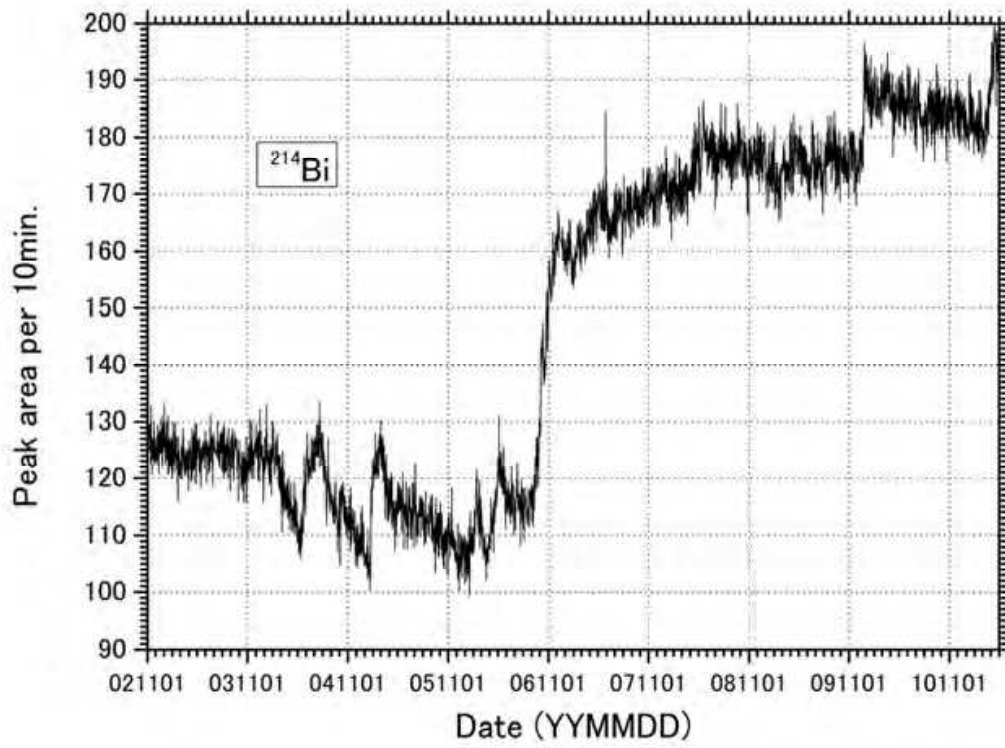


Fig. 11. Temporal change of the FWHM of respective peak: (a) ^{214}Bi , (b) ^{40}K and (c) ^{208}Tl .

By using those results, long term fluctuation of net area of each peak, which corresponds to each radiation dose rate, was calculated by using the same fitting function. Here, 30 day simple moving average of the above result on the centre position of the peak was used for p and the average of whole period on the FWHM (3.23, 5.97 and 8.10 for ^{214}Bi , ^{40}K and ^{208}Tl , respectively) was used as known variables in the equation, while A , a and b were the unknown parameter. The net area of each peak S is obtained by the following equation.

$$S = A \cdot \text{FWHM} \cdot \sqrt{\pi / \ln 2} / 2 \quad (2)$$

The respective result for ^{214}Bi , ^{40}K and ^{208}Tl is shown in Fig. 12.



IntechOpen

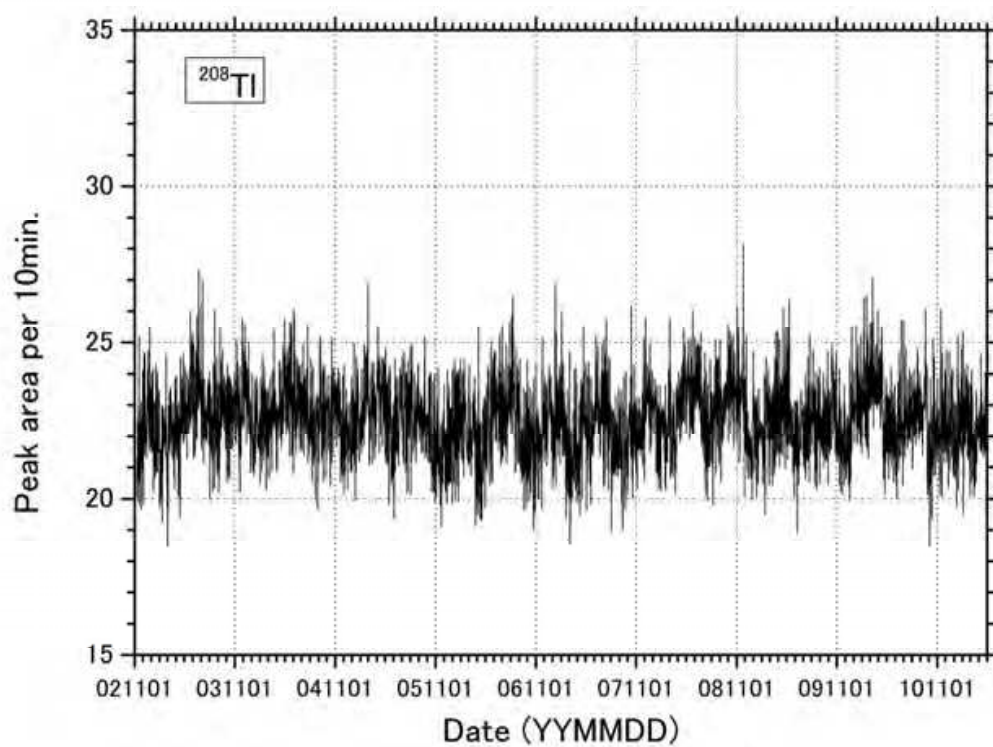


Fig. 12. Temporal change of the respective peak area; (a) ^{214}Bi , (b) ^{40}K and (c) ^{208}Tl .

In Fig. 12 (a), significant increase of ^{214}Bi peak area was observed in October 2006. The reason of this fluctuation is under study at present, though it may suggest the fluctuation of seepage or may reflect some tectonic deformation. Another increases which are less significant than that in October 2006 were observed several times, many of which seem to occur in spring. Since the increase of the amount of suspended materials have been also observed in spring, those may have some relation. In Fig. 12 (b), steady increase is observed. Although the reason is yet to be investigated, it may be caused by instrumental reason, e.g drift. Episodic increase of ^{40}K peak area was observed when M5.8 earthquake occurred east off Izu Peninsula on April 21st in 2006 which caused mudflow (Iwase et al, 2007). When M5 class earthquakes occurred on December 17th and 18th in 2009, increase of ^{40}K peak area seems to be less significant. This difference suggests the difference of mudflow composition as their suspended materials. The peak area of ^{208}Tl seems to be constant, though it contains somewhat periodical fluctuation which is caused by some error in calculation. Main reason is the selection of ROI (Range of Interest) channel for curve fitting calculation. While the variable p (the centre position of peak) in fitting function is fractional channel number, ROI is not, and then some discontinuity in the result occurs. Those preliminary results need much detailed evaluation in both technical and other environmental aspects.

5. Prospect and concluding remarks

One of the ways to improve the current model as for the proto-type apparatus is to develop stand-alone type of detector with battery and data logger system likely to an on-land system; it could deploy on the seabed for a year or more to accumulate the signals. Such a trial has already done by Ashi et al. (2003). Alternatively, once 10-times higher sensitivity of sensor achieved, such an apparatus may become quite powerful tool to monitor the rapid change of gamma ray intensities in deep sea environment, e.g. vibration of hydrothermal venting, tidal change of seepages. An application of plastic scintillator partly replacing the pressure hull is one of the available solutions (Shitashima et al., 2009).

6. Acknowledgments

All operations at sea had been supported numerous supports of captains, crews of research vessels, operation teams of submersibles or ROVs and technicians. Throughout the development, the authors express their thanks to colleagues of Deep Sea Research Department of JAMSTEC.

7. References

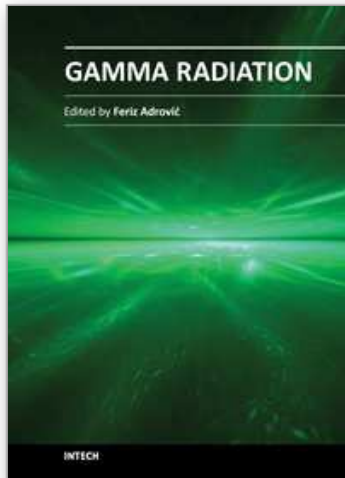
- Ashi, J., Kinoshita, M., Kuramoto, S.i., Morita, S. & Saito, S. (2003). Seafloor gamma ray measurements around active faults by standalone system, *JAMSTEC J. Deep Sea Research*, vol.22, pp.179-187 (in Japanese w/ English abstract)

- Bristow, Q. (1983). Airborne γ -ray spectrometry in uranium exploration- Principles and current practice, *The International Journal of Applied Radiation and Isotopes*, vol.34, No.1, pp.199-229
- Hattori, M., Kobayashi, Y. & Okano, M. (1997). Sea bottom radioactivity measurement systems in Japan, *Proc. 7th Internatl. Offshore and Polar Eng. Conf.*, vol.1, pp.116-119
- Hattori, M., Okano, M., & Togawa, O. (2000). Sea Bottom gamma ray measurement by NaI(Tl) Scintillation spectrometers installed on manned submersibles, ROV and sea bottom long term observatory, *Proc. 2000 International Symposium on Underwater Technology*, IEEE Catalog Number 00EX418, pp. 212-217.
- Hattori, M. & Okano, M. (2001). New results of sea bottom radioactivity measurement, *JAMSTEC J. Deep Sea Res.*, vol.18, pp.1-13 (in Japanese w/ English abstract)
- Hattori, M. & Okano, M. (2002). Sea bottom gamma ray measurement - Results of study and modeling of sea bottom radioactive environment -, *JAMSTEC J. Deep Sea Res.*, vol.20, pp.37-52 (in Japanese w/English abstract)
- Ito, T., Kinoshita, M., Saito, S., Machiyama, H., Shima, S., Gasa, S., Togawa, O. & Okano, M. (2005). Studies on Applications of Detectors for Marine Radioactivity and Methodologies for Data Analysis (Joint Research), *JAERI-research 2005-028*, pp. 127, Japan Atomic Energy Research Institute, Ibaraki-ken, Japan.
- Iwase, R., Mitsuzawa, K., Hirata, K.; Kaiho, Y., Kawaguchi, K., Fujie, G. & Mikada, H. (2001). Renewal of "Real-time Deep Seafloor Observatory off Hatsushima Island in Sagami Bay", *JAMSTEC J. Deep Sea Research*, vol.18, pp.185-192 (in Japanese w/ English abstract)
- Iwase, R. (2004). 10 Year Video Observation on Deep Seafloor at Cold Seepage Site in Sagami Bay, Central Japan, *Proc. OCEANS'04 / TECHNO-OCEAN'04: 2200-2205*
- Iwase, R., Goto, T., Kikuchi, T. & Mizutani, K. (2007). Earthquake Accompanied by Mudflow Observed by a Cabled Observatory off Hatsushima Island in Sagami Bay in April 2006, *Proc. 2007 Symposium on Underwater Technology and Workshop on Scientific Use of Submarine Cables and Related Technologies*, pp.472-475
- Jones, D.G., Roberts, P.D. & Miller, J.M. (1988). The distribution of gamma-emitting radionuclides in surface subtidal sediments near the Sellafield plant, *Estuarine, Coastal and Shelf Science*, vol.27, pp.143-161
- Kumagai, H. & Okano, M. (1982). A portable scintillation spectrometer for environmental radiation measurements, *Reports of the Institute of Physical and Chemical Research*, vol. 58, No.1, pp.1-10
- Momma, H., Iwase, R., Mitsuzawa, K., Kaiho, Y. & Fujiwara, Y. (1998). Preliminary results of a three-year continuous observation by a deep seafloor observatory in Sagami Bay, central Japan, *Phys. of Earth and Planet. Inter.*, vol.108, pp.263-274
- Okano, M., Izumo, K., Kumagai, H., Katou, T., Nishida, M., Hamada, T. & Kodama, M. (1980). Measurement of environmental radiations with a scintillation spectrometer equipped with a spherical NaI(Tl) Scintillator, *Natural Radiation Environment III, Symposium Series DOE51 (CONF-780422)*, pp.896-911
- Shitashima, K. (2009) Development of in-situ radon sensor using plastic scintillator, CRIEPI Research Report, V08054, pp. 17

Yoshida, N. & H. Tsukahara (1987) A γ -ray spectral survey on giant clam colonies using the submersible Shinkai2000. *JAMSTEC J. Deep Sea Res.*, Vol.3, pp.105-112 (in Japanese w/English abstract).

IntechOpen

IntechOpen



Gamma Radiation

Edited by Prof. Feriz Adrovic

ISBN 978-953-51-0316-5

Hard cover, 320 pages

Publisher InTech

Published online 21, March, 2012

Published in print edition March, 2012

This book brings new research insights on the properties and behavior of gamma radiation, studies from a wide range of options of gamma radiation applications in Nuclear Physics, industrial processes, Environmental Science, Radiation Biology, Radiation Chemistry, Agriculture and Forestry, sterilization, food industry, as well as the review of both advantages and problems that are present in these applications. The book is primarily intended for scientific workers who have contacts with gamma radiation, such as staff working in nuclear power plants, manufacturing industries and civil engineers, medical equipment manufacturers, oncologists, radiation therapists, dental professionals, universities and the military, as well as those who intend to enter the world of applications and problems of gamma radiation. Because of the global importance of gamma radiation, the content of this book will be interesting for the wider audience as well.

How to reference

In order to correctly reference this scholarly work, feel free to copy and paste the following:

Hidenori Kumagai, Ryoichi Iwase, Masataka Kinoshita, Hideaki Machiyama, Mutsuo Hattori and Masaharu Okano (2012). Environmental Gamma-Ray Observation in Deep Sea, Gamma Radiation, Prof. Feriz Adrovic (Ed.), ISBN: 978-953-51-0316-5, InTech, Available from: <http://www.intechopen.com/books/gamma-radiation/environmental-gamma-ray-observation-in-deep-sea>

INTECH
open science | open minds

InTech Europe

University Campus STeP Ri
Slavka Krautzeka 83/A
51000 Rijeka, Croatia
Phone: +385 (51) 770 447
Fax: +385 (51) 686 166
www.intechopen.com

InTech China

Unit 405, Office Block, Hotel Equatorial Shanghai
No.65, Yan An Road (West), Shanghai, 200040, China
中国上海市延安西路65号上海国际贵都大饭店办公楼405单元
Phone: +86-21-62489820
Fax: +86-21-62489821

© 2012 The Author(s). Licensee IntechOpen. This is an open access article distributed under the terms of the [Creative Commons Attribution 3.0 License](#), which permits unrestricted use, distribution, and reproduction in any medium, provided the original work is properly cited.

IntechOpen

IntechOpen